Performance Characterization of Microwave-multiplexed Transition Edge Sensors for X-ray Synchrotron Applications

O. Quaranta, D. Yan, T. Madden, L. Gades, U. Patel and A. Miceli
Advanced Photon Source
Argonne National Laboratory
Lemont (IL), USA
oquaranta@anl.gov

D. Becker, D. Bennett, J. Hays-Wehle, G Hilton, J. Gard, B. Mates, C. Reintsema, D. Schmidt, D. Swetz, J. Ullom, and L. Vale
NIST
Boulder (CO), USA

***Abstract*—State of the art energy-resolving detectors for synchrotrons are required to take full advantage of the capabilities of these facilities. Most spectroscopic applications at x-ray beam-lines require energy resolutions of the order of $E/\Delta E$>1000 and high detection efficiencies, which is beyond the capabilities of both semiconducting detectors and wavelength-dispersive spectrometers. Transition Edge Sensors represent the best candidates for this role by providing high-energy resolution with non-dispersive operation, and with much higher photon-collection efficiency. Recently a novel readout scheme for TESs based on microwave resonators has been introduced by NIST that allows array scalability to high pixel counts. In this work, we describe its application to TESs for x-ray, with particular attention to the optimization of the readout settings. Parameters such noise, linearity and sampling rate represent the benchmarks of this characterization.**

Keywords—TESs; Microwave; SQUID; Resonators; Detectors; Superconducting

I. Introduction

While semiconductor pair-breaking detectors (e.g. silicon-drift detectors) are currently the workhorse for most spectroscopic applications at x-ray synchrotron beamlines, their resolution is fundamentally limited by the statistics of electron-hole pair creation. An increasing number of synchrotron experiments require energy resolution far beyond (i.e., $E/\Delta E$ > 1,000) what is achievable with these types of detectors. For these applications, wavelength-dispersive spectrometers are generally used, and they provide excellent energy resolution but are inefficient in the collection of the x-rays emitted from the sample.

Superconducting detectors represent the best viable alternative that can overcome the limitations of both these technologies. The very low noise levels and energy-dispersive nature of superconducting detectors make efficient use of every single x-ray photon.

Three types of energy-dispersive superconducting detectors exist today: Superconducting Tunnel Junctions (STJs), Kinetic Inductance Detectors (KIDs) and Transition Edge Sensors (TESs). STJs have achieved resolutions of ~10 eV up to 2 keV and per-pixel count rates several 1000 counts/s. Groups in the U.S. and in Japan have fielded STJ instruments with ~102 pixels at synchrotrons [1]. However, it has been challenging to achieve reasonable resolutions and stopping power at energies above 2 keV. Furthermore, no efficient multiplexing scheme exists that allows for the scalability to larger arrays. Kinetic Inductance Detectors (KIDs) for x-rays come in two flavors: quasiparticle breaking [2] and microcalorimeters (i.e., Thermal Kinetic Inductance Detectors, TKIDs) [3]. Both technologies share a powerful microwave-multiplexed readout for scalability to larger arrays. Instruments with thousands of pixels have been already deployed for other wavelengths [4]. However, it has been challenging to reach energy resolutions better than 75 eV at 6 keV [3,5]. TESs have demonstrated energy resolution as good as 1.6 eV at 5.9 keV and 0.9 eV at 1.5 keV [6]. TES arrays with near unity quantum efficiencies > 100 keV have been demonstrated [6]. Currently the TES represents the best option in terms detection efficiency, energy resolution, and scalability. Complete soft x-ray TES spectrometers have been deployed at several USA synchrotron facilities (NSLS, APS, SSRL) but are not yet in widespread use. The main reason is the low count rate performance of the current generation of TES spectrometers. Count rate performance can be improved by increasing the size of TES arrays and increasing the speed of each pixel with correspondingly higher bandwidth readout systems. The current generation of x-ray TES spectrometers uses Time Domain Multiplexing (TDM) [6]. In this work, we characterize a TES multiplexing readout, which is meant to greatly improve count rate limits of TDM-readout x-ray TES arrays.

II. Microwave SQUID Readout

Recently, NIST has pioneered a new readout technology based on probing SQUID amplifiers with microwave probe tones and cryogenic microwave resonators that increases the measurement bandwidth of the multiplexed TES by three orders of magnitude [7]. Each TES detector of the array is coupled to a superconducting circuit (called a microwave multiplexer or "μmux" chip) composed of a SQUID amplifier

This work was supported by the Accelerator and Detector R&D program in Basic Energy Sciences Scientific User Facilities Division at the Department of Energy. This research used resources of the Advanced Photon Source and Center for Nanoscale Materials, a U.S. Department of Energy Office of Science User Facilities operated for the DOE Office of Science by Argonne National Laboratory under Contract DE-AC02-06CH11357.

and a microwave resonator (Fig.1). The TESs are multiplexed in frequency via the corresponding resonator frequency. The high bandwidth of each resonator and the total bandwidth available via the frequency multiplexing should allow for faster sensors and much larger arrays. In addition, all the SQUIDs have a common modulation [8], which enables large arrays to be read out via a pair of coaxial cables and few DC lines for SQUID modulation and TES biasing. The photon absorption in a TES causes a temporary variation in the TES current. This is coupled to the SQUID via the coupling inductance, which amplifies this variation. This much bigger current will then induce a measurable shift in the superconducting resonator frequency, via the inductive coupling between the SQUID and the resonator. By monitoring this variation, it is possible to measure the energy of the absorbed photon. Because of the periodic response of the SQUID, a linearization mechanism is needed. In conventional TDM this is done by the use of an active feedback loop that maintains the SQUID at the point of maximum sensitivity. This solution is here inapplicable because it would require the use of two wires per SQUID, defying the entire purpose of this new technology. Instead, in this technology a periodic ramp that sweeps through the multiple quanta in the SQUID is applied (Fig.2.a) [8]. If the ramp rate is much higher than the TES current pulse time constant, then these will look like a phase shift in the SQUID response to the ramp. Consequently, there will be direct proportionality between the TES current and the induced phase shift in the modulation, in our case: 9μA/phase period in the SQUID. This solution allows for the use of a single flux ramp line common to all the SQUIDs.

III. Demodulation Optimization

The flux ramp modulation scheme ideally requires an infinitely long voltage ramp across the flux modulation inductance. In reality only a saw tooth signal can be used. Intrinsic to the saw tooth signal is a reset edge, which inevitably has some finite time duration. During this reset, flux modulation is adversely affected, and this can introduce some non-ideality in the TES signal reconstruction. In Fig.2.a is an example of a measured phase modulated by the flux ramp signal, with two ramps present. In the center of the window, the reset between the two ramps and the consequent effect on the phase is clearly visible. In this section, we analyze the effect of parameters as number of oscillations in one ramp (N_{OSC}, which is proportional to the flux ramp amplitude), ramp frequency (F_{RAMP}) and number of oscillations used on the flux modulation (N_{USED}). We used two different measures as benchmarks for our analysis: System Noise Level (*SNL*), and System Linearity (SL).

For *SNL*, we measured the flux ramp-demodulated noise spectrum of a TES in the superconducting state. The spectrum has two main components. At low frequency, the Johnson noise from the shunt resistor in the TES bias circuit dominates the spectrum. At frequencies above the cutoff frequency of the shunt resistor and the TES coupling inductance, the μmux noise dominates the spectrum. For our analysis, we considered only the noise level above the cutoff frequency (at ~1 kHz).

For *SL*, we measured the linearity of the system by calculating the residual to a linear fit of the normal state branch

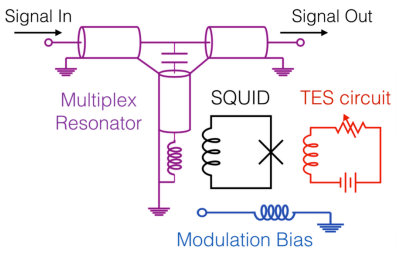

Fig. 1. Microwave SQUID multiplexer circuit. In red are represented the TES chips with their DC bias and the coupling inductor to the SQUID circuit. The SQUID circuit is then inductively coupled to the superconducting resonator. All the resonators are biased and read via a common microwave line, on which is also present a low temperature HEMP amplifier (not shown in figure). A common flux ramp line is also present.

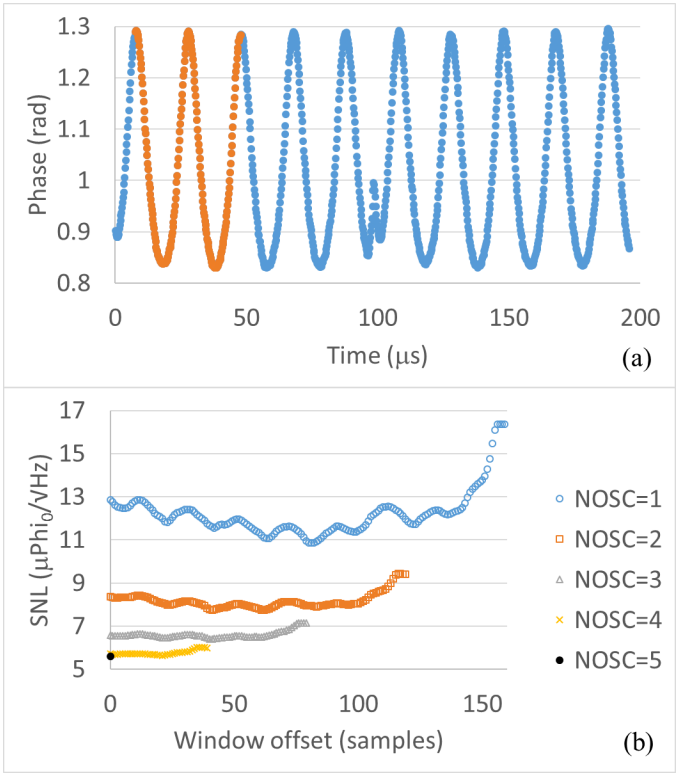

Fig. 2. (a) SQUID response to two ramps of flux modulation and highlight of an example of window selection. (b) *SNL* for different N_{OSC} and for different selection window postions.

of the current-voltage characteristic of a TES, and then selected the maximum peak-to-peak value.

Though these measurements were performed on three different x-ray TESs, for brevity, we present the results for only one TES that is representative of the other two devices as well. In Fig.2.a is represented the modulated signal on which we performed the analysis. The phase signal is composed of N_{OSC} = 5 SQUID oscillations including the effect of the ramp reset (from now on called "the glitch"), which set the SQUID modulation rate at $F_{MOD} = N_{OSC} \times F_{RAMP} = 50$ kHz. The single phase shift (TES current) value can be extracted by either considering the entirety (blue in Fig.2.a) or just a subset (orange in Fig.2.a) of the SQUID oscillations in a single ramp.

In Fig.2.b is represented the system noise level measured for different portions of the five phase oscillations: from N_{USED} = 1 up to N_{USED} = 5 (which includes the glitch). For each set of measurements, the oscillations selection window moves across the entire dataset starting from the left side. The *SNL* depends strongly on the window size. For shorter windows the *SNL* is generally higher (up to a factor 2) than for the longer windows. Moreover, shorter windows tend to have a *SNL* strongly dependent on the position in the ramp. The best *SNL* is achieved when at least four oscillations are considered and the level is quite constant regardless of the position in the ramp. Above this, the noise seems to saturate to *SNL* = 5 $\mu Phi_0/\sqrt{Hz}$ in the case of N_{USED} = 5, essentially identical to the case N_{USED} = 4. The effect of the glitch is quite evident in the case of shorter selection windows, due to the higher relative weight. For four and five oscillations, the inclusion of the glitch in the data set has little to no effect at these noise levels. Measurements of similar μmux chips at NIST have *SNL* a factor 2 lower than those measured at ANL. This discrepancy likely is due to lack of wire bonds from the ground plane on the SQUID input side of the μmux chip to the sample box, which results in anomalously low resonator quality factors.

A similar analysis was performed on the *SL*. The *SL* depends on both the selected window size and window position in the ramp, in a fashion similar to the *SNL*. *SL* is generally lower for wider selection windows and heavily dependent on the window position for small windows. On the other hand, the effect of the glitch is more dominant in the case of the *SL*: *SL* in the case of five oscillations is 0.025 Phi_0, while in the case of four oscillations is 0.024 Phi_0. *SL* for all the other cases is much higher. The conclusion of this analysis is that for our benchmark with F_{RAMP}=10 kHz and N_{OSC} = 5 the best demodulation setting is a four-oscillation window that rejects the last oscillation and the glitch.

In black in Fig.3 is represented a TES pulse generated by the absorption of an x-ray from a Fe-55 source, measured with these settings. The TES used in the test is a typical 6 keV x-ray TES from NIST: Mo/Cu bilayer with T_C = 105 mK, R = 8.8 mΩ normal state resistance and evaporated Bi absorber. The bias setup includes a R_{SHUNT} = 300 μΩ shunt resistor and L = 690 nH total inductance. From the figure, the poor of resolution in the rise time is evident, due to the low sampling rate set by F_{RAMP}. This can deteriorate the overall energy resolution. In purple a similar pulse is obtained with a F_{RAMP} = 100 kHz. In this case, the rise time is resolved very well and therefore determines the required sampling rate for this type of TES.

The current generation of μmux chips is composed of resonators of 300 kHz bandwidth. This poses a strong limit to the usable flux modulation frequency F_{MOD}. In fact, when we tried to operate the μmux chips with F_{MOD} > 100 kHz, either by increasing F_{RAMP} or N_{OSC}, both the *SNL* and *SL* performances worsened. The only acceptable configuration for such high sampling rate is F_{RAMP} = 100 kHz and N_{OSC} = N_{USED} = 1. In this case *SL*=0.039, while the *SNL* is comparable to the best *SNL* obtained with F_{RAMP} =10 kHz, N_{OSC} = 5 and N_{USED} = 4. With F_{RAMP} = 100 kHz and N_{OSC} = N_{USED} = 1 the baseline noise level predicts an energy resolution of ~ 4 eV for 5.9 keV. We expect this to improve with better wire bonding of the μmux ground planes.

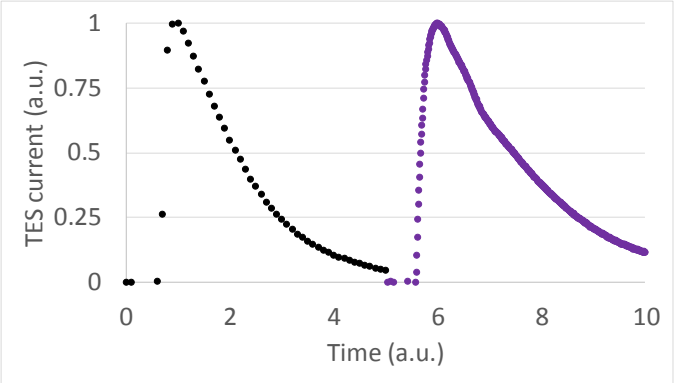

Fig. 3. TES pulse from a Fe-55 x-ray photon at F_{RAMP} = 10 kHz (black) and F_{RAMP}=100 kHz (purple).

IV. Conclusions

In this work, we described the use of a new readout technology for TESs developed at NIST based on the use of superconducting microwave resonators in combination with SQUID amplifiers. We studied its performance when used to read out x-ray TESs. The results provide a benchmark for the optimization of the technology performance and the "optimal" operation conditions for x-ray TESs. We are currently working on a 100-pixel hard x-ray TES demonstration using the μmux readout. The current limitations for these applications come from the limited bandwidth of the resonators used. NIST is currently working on newer versions of the μmux chip with 2 MHz bandwidth per channel to read out even faster TES devices.

References

[1] S. Friedrich et al., "New Developments in Superconducting Tunnel Junction X-Ray Spectrometers for Synchrotron Science," J. Low Temp. Phys., vol. 167, pp. 741-747, June 2012.

[2] B.A. Mazin, B. Bumble, and P.K. Day, "Position sensitive x-ray spectrophotometer using microwave kinetic inductance detectors," Appl. Phys. Lett., vol. 89, pp. 222507-1-3, November 2006.

[3] O. Quaranta, T.W. Cecil, L. Gades, B.A. Mazin, and A. Miceli, "X-ray photon detection using superconducting resonators in thermal quasi-equilibrium," Supercond. Sci. Technol., vol. 26, pp. 105021-1-6, September 2013.

[4] B.A. Mazin et al., "ARCONS: A 2024 Pixel Optical through Near-IR Cryogenic Imaging Spectrophotometer," Publ. of the Astron. Soc. Of the Pacific, vol. 125, pp. 1348-1361, November 2013.

[5] G. Ulbricht et al., "Highly multiplexible thermal kinetic inductance detectors for x-ray imaging spectroscopy," Appl. Phys. Lett., vol. 106, pp. 251103-1-4, June 2015.

[6] J.N. Ullom, and D.A. Bennett, "Review of superconducting transition-edge sensors for x-ray and gamma-ray spectroscopy," Supercond. Sci. Technol., vol. 28, pp. 084003-1-36, July 2015.

[7] J.A.B. Mates, G.C. Hilton, K.D. Irwin, and L.R. Vale, "Demonstration of a multiplexer of dissipationless superconducting quantum interference devices," Appl. Phys. Lett., vol. 92, pp. 023514-1-3, January 2008.

[8] J.A.B. Mates, K.D. Irwin, L.R. Vale, J. Gao, and K.W. Lehnert, "Flux-Ramp Modulation for SQUID Multiplexing," J. Low Temp. Phys., vol. 167, pp. 707-712, February 2012.